

MEASUREMENT OF THE ELECTRON-DEUTERON  
ELASTIC SCATTERING CROSS SECTION  
IN THE RANGE  $0.8 \leq q^2 \leq 6 \text{ GeV}^2$

R. G. Arnold, B. T. Chertok, E. B. Dally<sup>†</sup>, A. Grigorian<sup>‡</sup>,  
C. L. Jordan<sup>‡</sup>, W. P. Schütz, and R. Zdarko<sup>‡</sup>

American University\*  
Washington, D. C. 20016

and

F. Martin  
Stanford Linear Accelerator Center\*\*  
Stanford University, Stanford, California 94305

and

B. A. Mecking  
Physikalisches Institut  
Universität Bonn, Bonn, West Germany

(Presented by R. G. Arnold)

ABSTRACT

We report preliminary results of elastic eD scattering at large momentum transfer performed at the Stanford Linear Accelerator Center using two high resolution spectrometers in coincidence. We deduce the deuteron structure function  $A(q^2)$  at 9 values of  $q^2$  from a comparison of elastic eD and eP coincident yields and the world's eP cross sections. These measurements extend the range of  $q^2$  by 4.5 over previous work, and in this new range  $A(q^2)$  is observed to approach  $1/q^{20}$  momentum dependence. Our results are in sharp disagreement with the meson exchange calculations, and they are in rough agreement with the nonrelativistic potential models, and they are in agreement with the predictions of the quark dimensional scaling model which pictures the deuteron as a bound state of 6 quarks at large momentum transfer.

---

<sup>†</sup> On leave: Naval Postgraduate School, Monterey, California 93940

<sup>‡</sup> Present address: Stanford University, HEPL, Stanford, California 94305

<sup>‡</sup> On leave: I. Physikalisches Institut, Tech. Hochschule, Aachen, West Germany

\* Research supported by the National Science Foundation (GP-16565)

\*\* Work supported by the U.S. Energy Research and Development Administration

(Presented at the 6<sup>th</sup> International Conference on High Energy Physics and Nuclear Structure. Los Alamos Scientific Lab., Los Alamos, N. M., June 8-13, 1975)

## INTRODUCTION

The deuteron is the simplest bound state in nuclear physics with the consequence that its structure and internal dynamics are of fundamental significance. The deuteron has an important role in nuclear particle physics as a spin 1, isospin 0 dibaryon target for the study of symmetries of the strong interactions, for the investigation of elementary phenomena with a variety of photon and hadron particle beams and as a quasi-free neutron target for investigations of neutron-proton differences at high energies. This elementary neutron-proton bound state is reasonably well understood out to a relative momentum of  $\sim 500$  MeV/c in terms of the one-boson exchange potential (OBEP) using the known spectrum and couplings of the pseudoscalar and vector mesons or in terms of phenomenological potentials derived from N-N phase shifts and the deuteron's electromagnetic currents. Historically since the discovery of this isotope of hydrogen in 1932 by Urey, each decade of subsequent work has been marked by significant progress in the interplay of experiment and theory toward unraveling the subtleties of the nuclear force.

We present preliminary results of the measurement of electron-deuteron elastic scattering in the interval  $0.8 \leq q^2 \leq 6$  GeV<sup>2</sup>. This investigation of the deuteron employed the by now classic technique of high energy electron scattering developed by Hofstadter and co-workers in the 1950's.<sup>1</sup> The measurements were performed at the Stanford Linear Accelerator Center using the electron beam in the range 5 to 19 GeV with average currents from 0.2 to 30 microamperes and using the three small-acceptance high-resolution spectrometers on a common pivot.<sup>2</sup> These unique capabilities available at SLAC made this experiment possible. This investigation significantly extends the boundary on the deuteron structure function  $A(q^2)$  beyond  $q^2 \approx 1.3$  GeV<sup>2</sup>.<sup>3</sup> The deuteron structure function is extracted from the standard one-photon exchange electron scattering cross section,

$$\frac{d\sigma}{d\Omega} = \frac{d\sigma}{d\Omega}_{\text{Mott}} \left( A(q^2) + B(q^2) \tan^2 \frac{\theta_e}{2} \right) \quad (1)$$

where the invariant momentum transfer in terms of the electron's variables is  $q^2 = 4 E_i E_f \sin^2 \theta_e/2$ .

In order, the sections of this paper contain the predictions for  $A(q^2)$ , a description of the measurements, analysis, and the preliminary results for  $A(q^2)$ , and the comparison with the theories.

## THEORETICAL PREDICTIONS

Processes which are used to describe e-D elastic scattering are displayed in Fig. 1. At low  $q^2$  ( $\ll M^2$ ), the impulse approximation diagram (Fig. 1a) is expected to dominate and calculations using nonrelativistic wave functions (satisfying OBEP with a depression in  $\psi$  for  $r < 1F$ ) are in good agreement with eD elastic scattering as well as a large body of other low energy data. The deuteron structure function  $A(q^2)$  determined by forward electron scattering is dominated by the charge and quadrupole distributions. For the spin-one deuteron, Gross<sup>4</sup> has shown that

$$A(q^2) = G_0^2 + \frac{8}{9} \eta^2 G_2^2 + \frac{2}{3} \eta G_1^2 \quad (2)$$

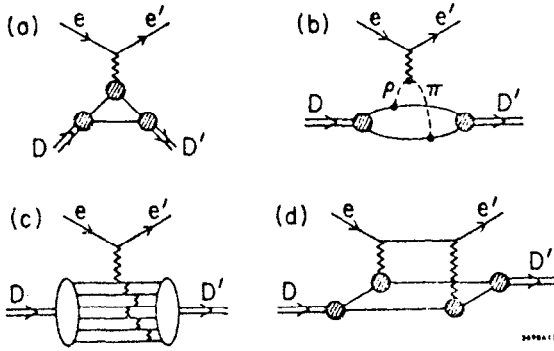


Fig. 1. Electron deuteron elastic scattering.

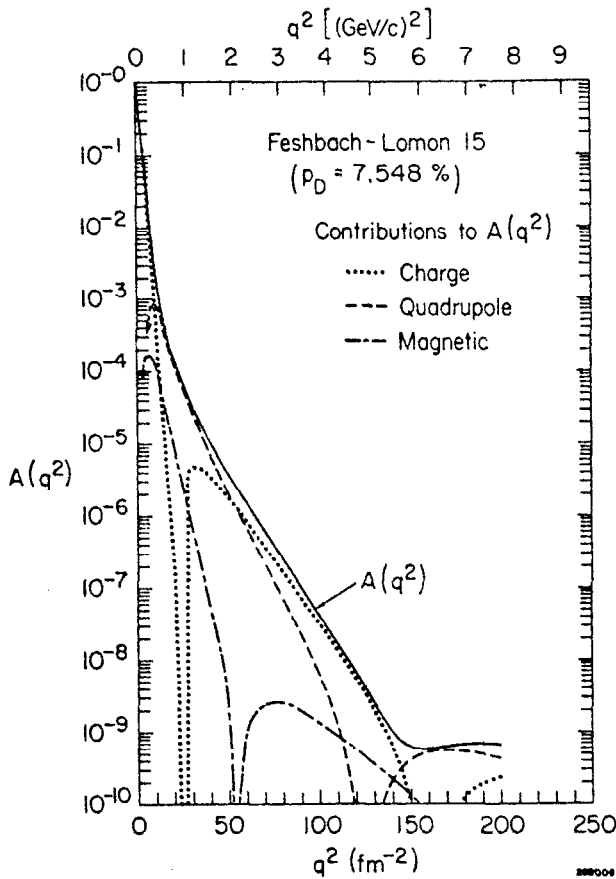


Fig. 2. Deuteron structure function  $A(q^2)$ .

At high momentum transfer, it was expected that mechanisms which share the momentum transfer approximately equally between the two nucleons would dominate the structure function. Otherwise the deuteron would break up when struck with a  $q > 350$  MeV/c. Three such momentum-

where  $\eta = q^2/4M_D^2$  and the  $G(q^2)$ 's are the charge, quadrupole, and magnetic form factors, respectively. Thus  $A$ , the deuteron structure function, is a composite of all of the deuteron's electromagnetic properties. The other term in Eq. (1),  $B(q^2)$ , the deuteron's magnetic structure function, is just a function of  $G_1$ . The individual terms in Eq. (2) are displayed in Fig. 2 for the impulse approximation prediction out to  $q^2 \sim 8$  GeV<sup>2</sup> (200 F<sup>-2</sup>);  $A(q^2)$  is calculated using empirical dipole fits for the nucleon form factors, i. e., with  $G_{EN} = 0$ , and using the boundary condition wave functions of Feshbach-Lomon (Potential #15 with the <sup>3</sup>D<sub>1</sub> state percentage of 7.55%).<sup>5</sup> Spherical Bessel functions  $j_0$  and  $j_2$  of argument  $qr/2$  modulate  $G_0$ ,  $G_2$ , and  $G_1$ . The magnetic term is small everywhere with a maximum contribution of 20% to  $A$  at  $q^2 \approx 5.8$  GeV<sup>2</sup>. The impulse approximation predictions using three nonrelativistic wave functions (FL-5 with  $P_D = 5.2\%$ , FL-15 and the Bethe-Reid Soft Core<sup>6</sup> with  $P_D = 6.5\%$ ) are given in Fig. 3. The differences in  $A$  are due to the differing percentages of tensor force and treatments of the interior of  $\psi$ .

Refinements to the deuteron wave functions from inserting isobars to give N-N'(1470) and  $\Delta$ - $\Delta$  (1236) admixtures, because of their high momentum components, are expected to increase  $A$  at high  $q^2$ . Similar contributions to  $A$  are expected from loops and oscillations in the interior of the deuteron wave function from a variety of postulated dynamics.<sup>7</sup>

equipartition diagrams are displayed in Fig. 1. Meson exchange currents (Fig. 1b) were expected to dominate  $A$  for  $q^2 \gg M^2$  and have been calculated by several groups. They used the meson degrees of freedom consistent with OBEP ( $\pi$ ,  $\sigma$ ,  $\rho$ ,  $\omega$ , etc.) and containing the proper quantum numbers and dynamics of the  $\gamma XX$  vertex -  $\gamma\rho\pi$ ,  $\gamma\omega\sigma$ ,  $\gamma NN\bar{\pi}$ , etc. The recent work of Chemtob, Moniz, and Rho<sup>8</sup> refined and extended the pioneering work of Adler and Drell;<sup>9</sup> they are in agreement that the  $\gamma\rho\pi$  and  $\gamma\omega\sigma$  exchange currents should dominate  $A(q^2)$  for  $q^2 \gg M^2$ . This meson exchange current prediction is displayed in Fig. 3 and shows an early flattening of  $A$  for  $q^2 \gtrsim M^2$ . Additional effects of pion-exchange pair (NN) and recoil currents have been calculated by Jackson, Lande, and Riska to boost  $A$  by a factor of 3 over the impulse approximation already at  $q^2 = 1.75 \text{ GeV}^2$ .<sup>10</sup> Thus theorists who are applying these meson exchange currents to an increasing variety of classical nuclear physics problems have predicted a dramatic flattening of  $A$  with increasing  $q^2$  beyond  $1 \text{ GeV}^2$ .

An alternative approach to sharing of  $q^2$  has been suggested by Blankenbecler and Gunion.<sup>11</sup> The photon-meson vertex is treated by vector dominance with the vector meson subsequently scattering from one nucleon and being absorbed by the other. This model, which introduces mechanisms understood to dominate at high energies, predicts the flattening of  $A$  shown in Fig. 3. The electromagnetic  $2\gamma$  mechanism shown in Fig. 1d is another candidate for sharing the momentum transfer to the two nucleons equally.<sup>12</sup> Observation of this effect would have important implications for high energy lepton scattering which is universally analyzed in the  $1\gamma$  approximation. As observed in Fig. 3, the predicted  $A$  from  $2\gamma$  exchange is still below the  $1\gamma$  result since the extra factor of  $\alpha^2$  ( $\sim 10^{-4}$ ) is not fully recovered by the deuteron wave function at zero-relative momentum.

The final approach toward understanding deuteron structure at large  $q^2$  takes the bold step of viewing the deuteron as a six-quark bound state. The nucleons and meson clouds are replaced by point-like constituents which share the momentum transfer roughly equally, i.e.,  $q/6$ , in the high energy collision with the virtual photon as displayed in Fig. 1c. The dimensional-scaling quark model of Brodsky and Farrar<sup>13</sup> has enjoyed substantial success in describing large momentum transfer dependences for both inclusive and exclusive reactions. They use a Bethe-Salpeter model for hadrons constructed of bound point-like objects and predict that the  $q^2$  dependence of

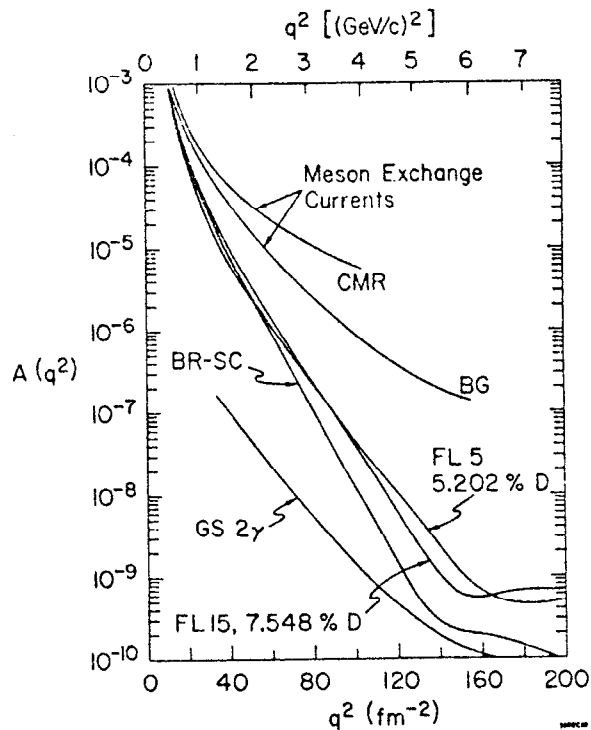


Fig. 3. Deuteron structure functions  $A(q^2)$ .

processes in the scaling region ( $s \gg q^2 \gg m^2$ ,  $s = \text{c.m. energy}$ ) is determined by the total number of constituent fields participating in the interaction. The hadron electromagnetic form factors are predicted to have the  $q^2$  dependence,

$$F_H \sim (q^2)^{1-n} \quad (3)$$

The momentum transfer  $q$  to the hadron must be partitioned among the constituent quarks to change their momentum along  $q$ , and roughly speaking there is one power of  $q^{-2}$  in the form factor from the propagator of each off mass shell quark. For  $n$  quarks there are  $n-1$  off shell in the coupling to the virtual photon. This model predicts

$$F_\pi \sim (q^2)^{-1} \quad (4)$$

$$F_{1P} \sim (q^2)^{-2} \quad (5)$$

in agreement with experiment for  $q^2 \gg m^2$ , where  $m$  is the mass of the hadron. For example,  $q^4 G_{MP}$  is a constant for  $q^2 > 4 \text{ GeV}^2$  as predicted. For the deuteron they predict

$$F_D \sim (q^2)^{-5} \quad (6)$$

where  $F_D = \sqrt{A}$ , meaning that  $A \sim q^{-20}$  for very large  $q^2$ . For the present measurement, Brodsky has suggested the form<sup>14</sup>

$$F_D \sim F_{1P}^2 \left( \frac{q^2}{4} \right) \left( 1 + \frac{q^2}{m^2} \right)^{-1} \quad (7)$$

to observe the onset of the 5 powers of  $q^2$  below the scaling region. The effective mass  $m$  is  $\sim 1.0-1.7 \text{ GeV}$ , and  $F_{1P} = (1 + q^2/.71)^{-2}$ . Another form which might display the quark degrees of freedom at moderate  $q^2$  is

$$F_D \sim \left[ 1 + \frac{q^2}{36M_Q^2} \right]^{-5} \quad (8)$$

where the effective quark mass,  $m_Q$ , can be taken from the proton form factor ( $m_Q^2 = .71/9$ ). Equations (7) and (8) are useful to see whether the experiment is consistent with  $(q^2)^{-5}$  at momentum transfers where the 6 quarks are near their mass-shell values.

To summarize this section, the theoretical predictions for the  $q^2$  dependence of the deuteron structure function  $A(q^2)$  for  $q^2 \gg 1 \text{ GeV}^2$  are widely divergent. Classical nuclear physics, meson exchange current phenomenology, and the dimensional-scaling quark model take strikingly different views of short distance phenomena. Some of the predictions are displayed in Fig. 3.

## THE EXPERIMENT, ANALYSIS, AND RESULTS

Elastic electron deuteron scattering was measured at nine values of  $q^2$ , 0.8, 1.0, 1.5, 1.75, 2.0, 2.5, 3.0, 4.0, and 6.0  $\text{GeV}^2$ , using two spectrometers in coincidence for an enhancement in signal-to-noise over a single spectrometer ranging from 200 to 1000. The system was calibrated using eP elastic scattering and the eD cross section was determined by comparison with the coincident yield for eP scattering at each  $q^2$ . The accidental coincidence background was 20% of the elastic eD signal at  $q^2$  of 1  $\text{GeV}^2$  and decreased faster than the signal with increased  $q^2$  until above  $q^2$  of 2.5 there was no accidental background. This work demonstrates the feasibility of performing elastic coincidence experiments on a low duty cycle electron linac (the SLAC duty cycle is  $5 \times 10^{-4}$ ).

### APPARATUS

A schematic of the scattering geometry is given in Fig. 4. The primary electron beam with pulse length of  $1.5 \mu\text{s}$  was momentum-analyzed to  $\sim \pm 0.5\%$  in  $\Delta p/p$  and passed through a liquid hydrogen or deuterium target.

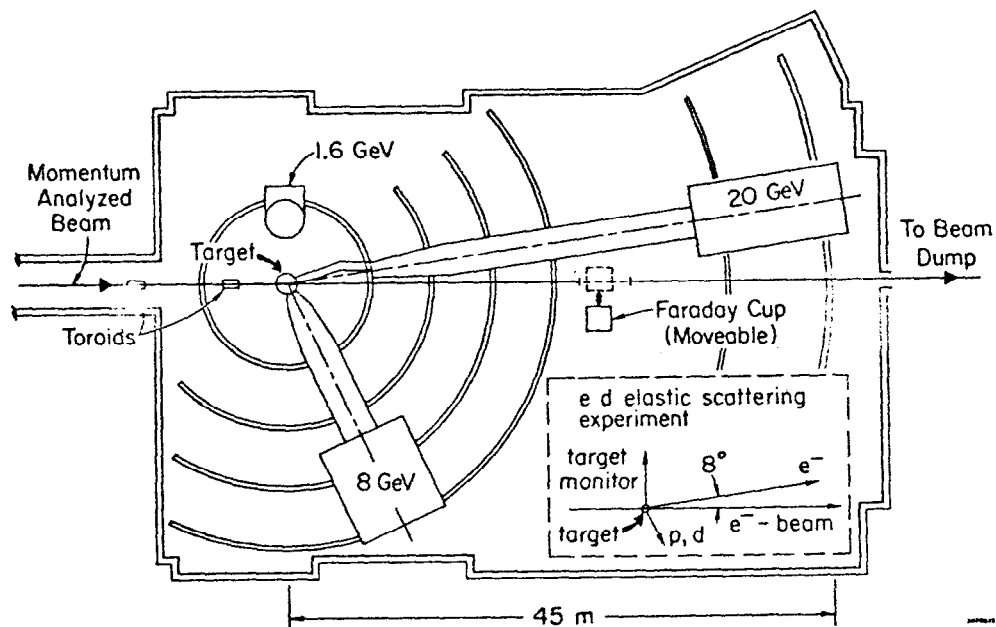


Fig. 4. End Station A.

The beam current was measured using the SLAC toroids. A Faraday cup was used to check the toroid calibration at regular intervals between runs. The uncertainty in the ratio of the total charge delivered to the targets was less than 1%.

The targets were identical 30 cm long Al cylinders 5 cm in diameter with .25mm side walls and .13 mm end caps in which liquid hydrogen and deuterium was circulated from reservoirs at  $21^\circ$  and 1.5 atm. Tests were made and no indication was found for changes in the target density due to bubbling of the liquid over the full range of beam power of this experiment.

The scattered electrons were detected in a spectrometer capable of analyzing particles up to 20 GeV/c momentum which was kept fixed at 8 degrees with respect to the incident beam. The recoil protons and deuterons were detected in the 8 GeV spectrometer which was moved from 75 to 53 degrees as  $q^2$  varied from 0.8 to 6 GeV<sup>2</sup>. These two spectrometers are high resolution multimagnet systems with separate momentum and scattering angle foci whose transport properties and acceptances have been studied carefully by various experimenters in the past few years. For our kinematics the 8 GeV spectrometer was the limiting aperture in  $\theta$  and  $\phi$  with an acceptance of roughly  $\Delta\theta \Delta\phi \Delta p/p = (.015)(.060)(.04)$  sr.

Scattered electrons were identified in the 20 GeV spectrometer with a two-fold scintillator coincidence plus a high pulse height from a lead glass and lead lucite total absorption shower counter (see Fig. 5a). Five planes

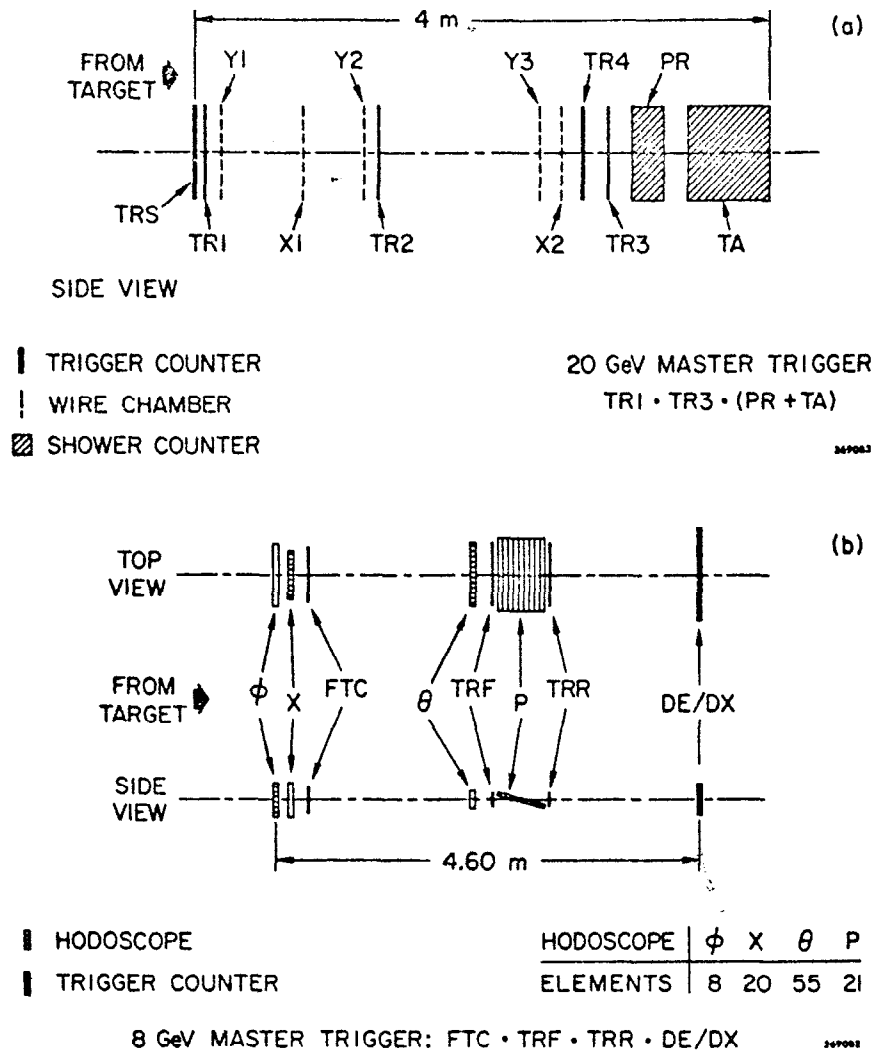


Fig. 5. (a) Counter arrangement in the 20 GeV spectrometer.  
(b) Counter arrangement in the 8 GeV spectrometer.

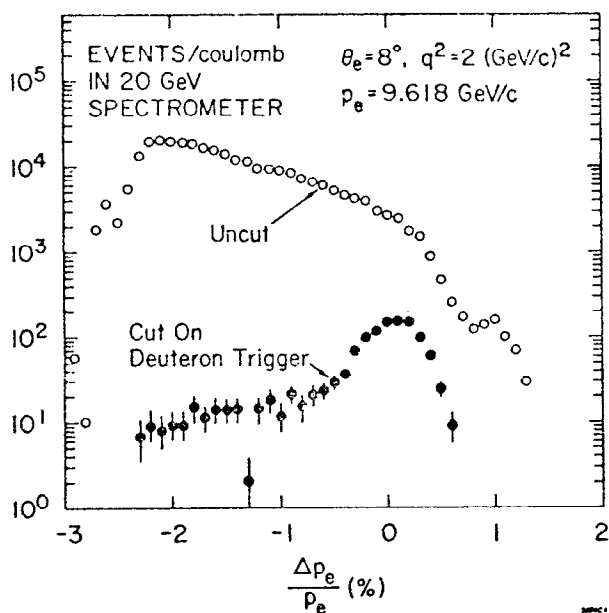


Fig. 6. Electron scattering from deuterons.

of proportional wire chambers were used for track reconstruction, and with the known spectrometer transport coefficients the momentum and scattering angles of the particles leaving the target were determined with resolution of  $\pm .05\%$  in  $\Delta p/p$  and  $\pm .05$  mr in  $\theta$  and  $\phi$ .<sup>15</sup> The full momentum acceptance of  $4\%$  in  $\Delta p/p$  of the scattered electrons included the elastic eD peak with a width of approximately  $\pm .3\%$  along with the upper portion of the quasielastic peak, as shown in Fig. 6. The quasielastic electrons accounted for nearly all the electron counting rate and were the main source of background in the 20 GeV arm. The charged pion background is insignificant near the elastic peak at  $8^\circ$  as determined by

the pulse height distribution in the total absorption counter.

The trigger for a good particle in the 8 GeV spectrometer was a four-fold scintillator coincidence (see Fig. 5b). This spectrometer was operated at momenta in the range 0.9 to 3 GeV and the primary counting rate in the eD measurements was due to large numbers of recoil protons from quasielastic electron scattering in the target. Approximately  $5\%$  of the 8 GeV single arm rate was due to pions. The 8 GeV spectrometer was also equipped with four planes of scintillator hodoscopes which were used for track reconstruction for those events with one unambiguous track with resolution of 0.3 mr in  $\theta$  and 0.2% in  $\Delta p/p$ .<sup>16</sup> Using the measured tracks of the momentum analyzed particles and the known transport properties of the two spectrometers, the double arm missing mass resolution was 10 MeV for 10 GeV incident electrons. The 4.3 m flight path between the first and last scintillators in the 8 GeV detector system made possible identification of pions, protons, and deuterons by time of flight (TOF); protons and deuterons were separated up to  $q^2$  of 3 GeV<sup>2</sup>. The information from the 8 GeV hodoscopes and from TOF inside the 8 GeV arm was used to give confidence in the double arm time-of-flight identification of elastic eD events, described below. The eD elastic signal was clearly established in the double arm TOF and any further cuts would have made a small improvement in the signal-to-noise at the price of making corrections for the inefficiencies of those cuts.

The eD elastic events were identified by recording the relative time of flight of particles causing triggers in the two spectrometers. The electron trigger was used for the start and the deuteron trigger for the stop in a 1024-channel time-to-digital converter. One such double arm TOF spectrum is displayed in Fig. 7. The peak represents the signal of double arm elastic eD events. The background of accidental coincidences is caused mainly by

electrons in the 20 GeV and protons in the 8 GeV system from separate quasielastic events in the target. The momentum and angle acceptance of the two spectrometers was small enough that true eP coincidences from quasielastic scattering were not accepted by the system. This accidental background was 20% of the eD coincidence peak height at  $q^2 = 1 \text{ GeV}^2$  and decreased at larger  $q^2$  until at  $q^2 = 2.5 \text{ GeV}^2$  and above the background was negligible. The accidental background in the eP TOF spectra was less than 1%.

This experiment would not have been possible using only one spectrometer. The top curve in Fig. 6 shows the momentum spectrum of scattered electrons at  $q^2 = 2 \text{ GeV}^2$  with no visible elastic peak and the large quasielastic signal rising at lower momenta out to the limit of the acceptance. The bottom curve in Fig. 6 and the curve in Fig. 8 on a linear scale show the momentum spectrum of electrons for those events in a time cut containing the double arm TOF peak in Fig. 7. The ratio of the area of the signal peak to the area of the uncut signal plus background in Fig. 6 is  $\sim 1/220$ . A similar situation existed in the recoil arm. The hatched area in Fig. 8

represents the momentum distribution of electrons for accidental events in a time cut placed below the eD TOF peak. Fig. 9 shows the eP and eD coincidence elastic peaks at  $q^2$  of  $1 \text{ GeV}^2$ , indicating the relative sizes of the eP and eD signals and the comparable peak shapes. The eP and eD coincident counting rates used in this analysis were determined from the areas of the elastic peaks as in Fig. 9 after the accidental background was subtracted.

An XDS 9300 computer was used to monitor the hardware and analyze a sample of the data as it was being accumulated. The computer was

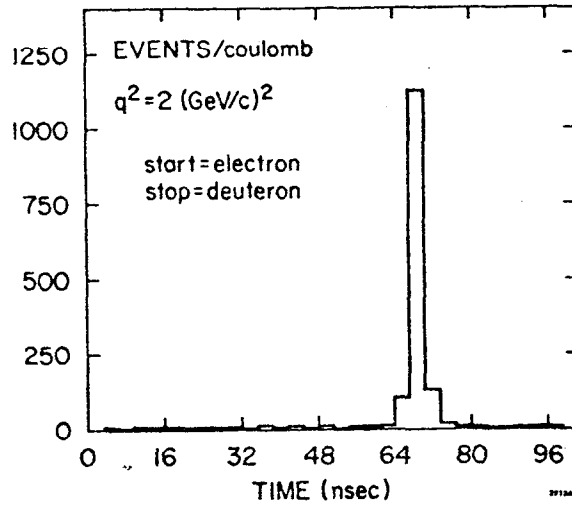


Fig. 7. Electron deuteron coincidence timing.

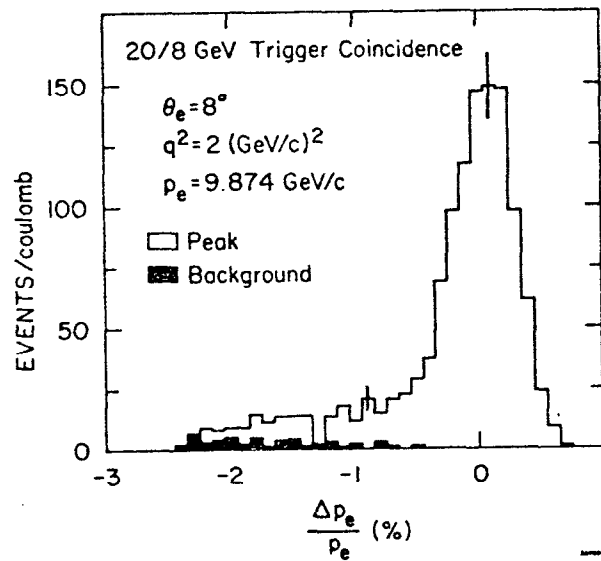


Fig. 8. Electron scattering from deuterons.

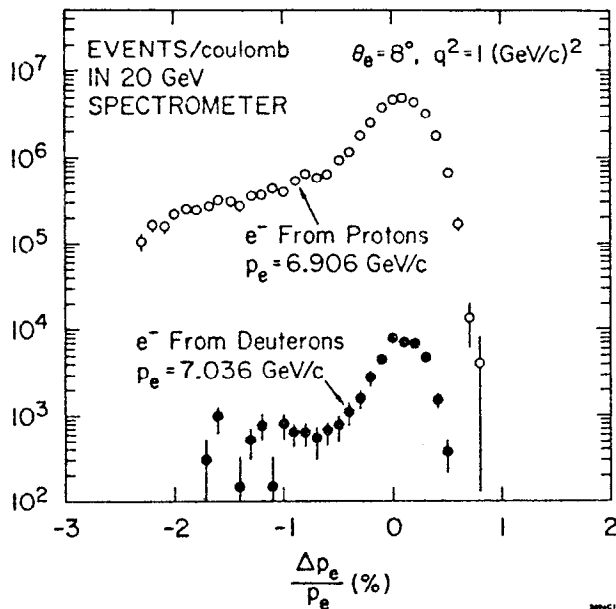


Fig. 9. Electron scattering from protons and deuterons.

sured interval in  $q^2$ . At  $q^2 = 6 \text{ GeV}^2$  no double arm coincidences were observed for 1.9 coulombs of incident electrons. The 3 standard deviation upper limit for the cross section is  $d\sigma/d\Omega_D \leq 5 \times 10^{-40} \text{ cm}^2/\text{sr}$ . At this  $q^2$  the eD elastic coincident event rate is estimated at 1 event per week at full SLAC beam power, with an accidental rate of 1 event per 5 to 10 years.

The ratio measurements we report have the advantage that most of the important properties of the detection system that affect the coincidence counting rate do not change or change very little for the conditions of eP and eD scattering. Using the corrections described below, the absolute eP cross sections have also been extracted for all  $q^2$ . They agree with the world average cross sections<sup>17</sup> within the estimated 20% uncertainty of the absolute measurement, which lends additional support to our confidence in the ratio results. The important corrections used to extract cross sections are as follows:

1. Dead time. The dead time of the trigger system was kept below 10% by adjusting the beam current and was accurately measured.
2. Inefficiency of the 8 GeV trigger. Deuterons and protons are absorbed and scattered differently by nuclear collisions in the scintillator material in the 8 GeV detector system (total path length,  $8.5 \text{ gm}/\text{cm}^2$ ) contributing to different losses of elastic events from the proton and deuteron triggers. These effects have been studied experimentally using the single arm 8 GeV data and we have calculated the effect using elastic and inelastic cross sections from the literature. The ratio of proton to deuteron absorption losses is  $1.10 \pm 0.05$  for all values of  $q^2$ .
3. Solid angle variation. To measure eP and eD scattering at the same  $q^2$  the electron scattering angle was kept fixed at  $8^\circ$  while the beam energy, spectrometer momenta, and recoil angle were adjusted. This change in the

alerted for single arm electron and deuteron and double arm coincidence triggers, and all event information was logged on magnetic tape for later study. The current in the power supplies for the 17 spectrometer magnets was continuously monitored and kept stable to one part in  $10^4$ .

## ANALYSIS

The deuteron elastic cross section at each  $q^2$  was determined from the ratio of the deuteron to proton coincidence yields, times the ratios of correction factors discussed below, times the world's average proton cross section. The deduced deuteron cross section was observed to decrease by a factor of about 200,000 over the mea-

recoil angle (from 10 to 20 degrees) made small changes in the angular acceptance. The double arm acceptance is determined by the vacuum pipe and detectors of the 8 GeV spectrometer. To determine the ratio of the double arm acceptance for eP to eD scattering we have constructed a detailed Monte Carlo model which includes: the transport coefficients for both spectrometers determined from previous work,<sup>18</sup> events with elastic kinematics, a spread on the incident beam energy, internal and external soft photon radiation from the incident and scattered electrons in the target material and windows, multiple coulomb scattering of the recoil particles, and the geometry of all slits, vacuum pipes, and detectors of our configuration. Using this model we determined the ratio of the deuteron to proton acceptance to be approximately 1 at  $q^2$  of 1 GeV<sup>2</sup> growing to 1.3 at  $q^2$  of 6 GeV<sup>2</sup>. We estimate the uncertainty of this ratio to be less than 10%.

4. Radiative corrections. The radiative corrections to elastic scattering where the recoil target particle and the scattered electron are detected in coincidence are more complicated than that for the case where only the scattered electron or the recoil particle is detected. For coincidence detection the phase space for the undetected photons is restricted and the boundaries for the phase space integrals depend on the details of the kinematics and the detector acceptances of a given experiment. We have done a numerical evaluation of the effect of soft photon radiation<sup>16</sup> for our precise geometry and kinematics using the double arm Monte Carlo, and we find that the ratio of the radiative corrections for eP and eD scattering with coincidence detection is  $1.00 \pm 0.05$  for all  $q^2$  of this experiment.

The important corrections to the individual counting rates which divide out of the ratio include: trigger inefficiency of the electron detector ( $\sim 1\%$ ); track inefficiency of the wire chambers in the 20 GeV spectrometer ( $\sim 10\%$ ); absolute normalization of the charge measured by the toroids (1%).

## RESULTS

The results for the deuteron structure function  $A(q^2)$  deduced from our measurements are presented in Fig. 10, along with current theoretical predictions. The experimental uncertainty in the ratio method is thought to be less than 12%. The error bars on the data points in Fig. 10 represent the statistical errors, the error on the world's eP cross sections, and the approximate 12% uncertainty in the ratio measurement added in quadrature for this preliminary report. The error bar at  $q^2 = 6$  GeV<sup>2</sup> represents a 1-standard deviation limit.

## INTERPRETATION OF RESULTS

The structure function is observed to decrease rapidly and smoothly by  $\sim 10^4$  in the interval 1 to 6 GeV<sup>2</sup>. The meson exchange current predictions are completely contradicted by this experiment, i.e., instead of dominating at high  $q^2$  they appear to be absent. This conflict of experiment and theory is particularly significant because of the rapidly developing application of meson exchange current calculations in nuclear physics.

Some of the possible reasons for complete failure of the exchange current predictions are enumerated.

1. This disagreement may arise from the isoscalar nature of the deuteron's electromagnetic current ( $\Delta T = 0$  implies an odd number of pions

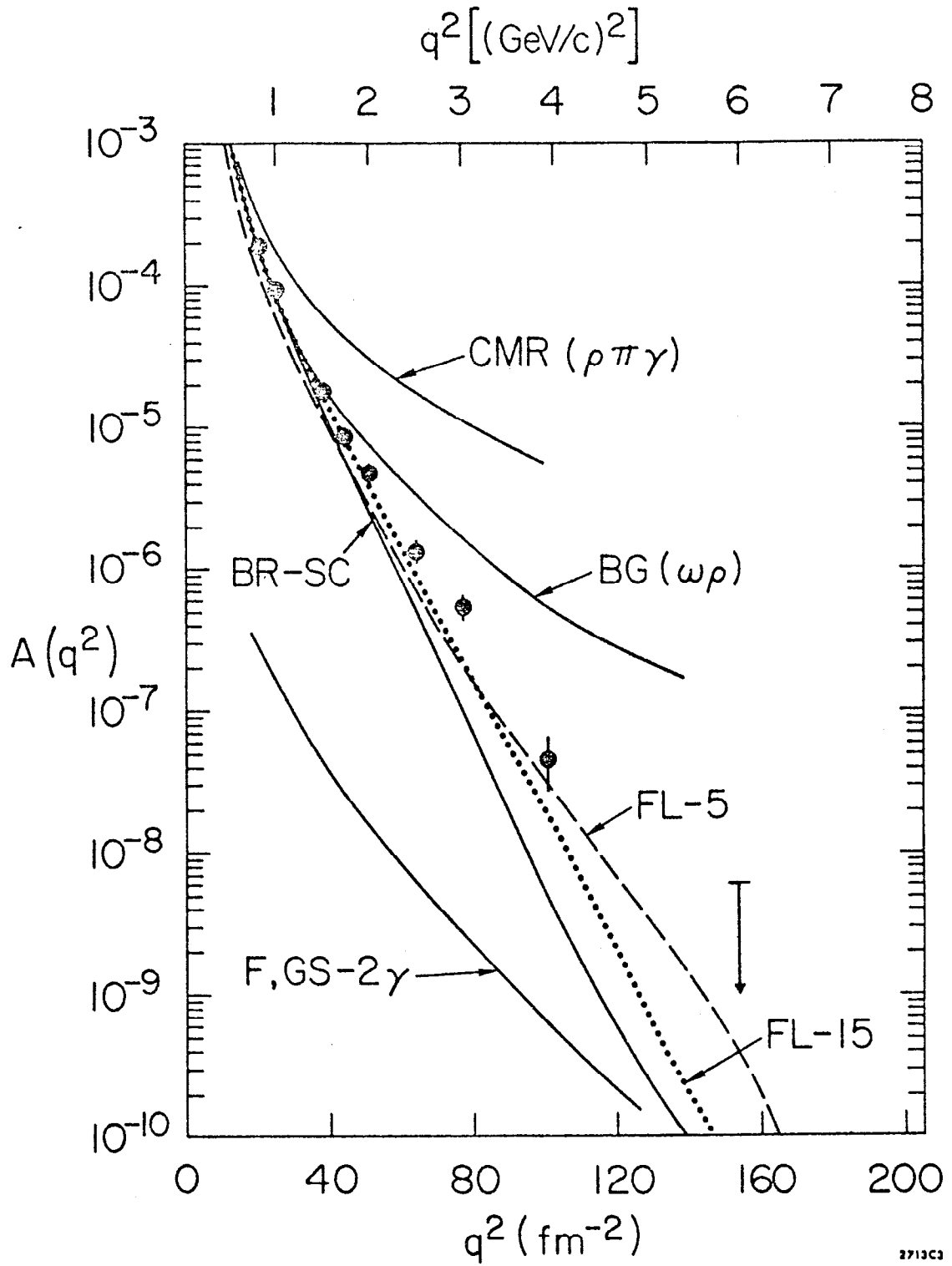


Fig. 10. Deuteron structure function  $A(q^2)$ .

at the virtual photon-meson vertex).

2. It may be a violation of SU(3) symmetry so that the decay  $\rho \rightarrow \pi\gamma$  is strongly suppressed. The comparison in Fig. 10 with CMR yields  $\Gamma_{\rho\pi\gamma} \lesssim 0.25/100$  MeV where 0.25 MeV was used as an upper limit on the decay width by CMR. Similar implications apply to the existence of the radiative decay  $\omega \rightarrow \sigma\gamma$ .

3. It may arise from the very rapid weakening of vector-meson dominance of the photon as its mass becomes large, i. e.,  $m_\gamma^2 = q^2$ .<sup>11</sup>

4. It may arise from subtle cancellations in diffractive amplitudes<sup>11</sup> as the meson propagates from one nucleon to the second one.

5. It could be that quarks rather than mesons and nucleons are the important degrees of freedom at large  $q^2$ .

The recent measurement<sup>19</sup> of the decay width  $\Gamma_{\rho\pi\gamma} = 35 \pm 10$  keV decreases the CMR prediction by  $\sim \frac{1}{4}$  at  $q^2 = 4$  GeV<sup>2</sup> for  $A(q^2)$  so that this prediction is still 25 times greater than experiment.

The predictions of the nonrelativistic potential models indicated in Fig. 10 are in rough agreement (within factors of 2 to 10) with the results of this experiment. Other NN potentials may also fit the high  $q^2$  behavior of  $A(q^2)$ . However, very low  $q^2$  eD elastic data favors the potential FL-15 with the BR-SC and FL-5 being acceptable there at the 2 standard deviation level.<sup>20</sup> For those curves we have used the best fit nucleon form factors,  $G_{EP}$ ,  $G_{MP}$ ,  $G_{EN}$ , and  $G_{MN}$  in Equation(2).<sup>21</sup> At this time we do not want to distinguish between the various potential models because of the theoretical work required on relativistic corrections or a relativistic theory of the NN interaction.<sup>22</sup> The relativistic corrections now available are presented as expansions in powers of  $q^2/m^2$  and are not reliable above  $q^2 \sim 1$  GeV<sup>2</sup>. We can say, based on the rough agreement of the nonrelativistic models with our data, that such corrections are smooth and probably smaller than a factor of 2 to 10 out to  $q^2$  of 4 GeV<sup>2</sup>. Since  $G_{EN}$  contributes about 60% to  $A(q^2)$  in the impulse approximation, it may be possible, using the best available deuteron wave functions with relativistic corrections, to extend the information on the neutron form factor in the further analysis of our data.

Isobar admixtures and short range forbidden states have been speculated to reside in the deuteron.<sup>7</sup> To the extent that both of these mechanisms give significant high-momentum components to the deuteron wave function that would flatten out  $A(q^2)$ , it can be observed in Fig. 10 that these theoretical speculations are made highly improbable by this experiment.

The deuteron viewed as a structure of 6 point-like quarks fits the observed falloff of  $A(q^2)$ . The  $(q^2)^5 F_D$  form in Eqs. (6), (7), and (8) applied to  $A(q^2)$  approaches a constant at relatively low values of  $q^2$  as displayed in Fig. 11 for Eq. (8). Indeed the premature approach to scaling at  $q^2 \approx .75$  GeV<sup>2</sup> (from Eq. (7)) has important implications for both the dimensional scaling quark model and for nuclear physics. This precocious scaling when the constituent quarks are near their mass-shell has been observed in other reactions and may be illuminating a new feature of the quark model or a new principle like high-energy duality.<sup>23</sup> The implications for nuclear physics are vast if quarks are the degrees of freedom at short distances in nuclei. This SU(3) content in the short distance behavior of the N-N interaction could show up in a variety of nuclear physics phenomena, particularly in view of this early appearance (at low  $q^2$ ) of 6-quarks in the deuteron.

It is beyond the scope of this paper to suggest whether the ability of both classical nuclear physics and the dimensional-scaling quark model to explain the large  $q^2$  dependence of the deuteron structure is an accident. We suspect that it is not an accident. This coincidence should be a significant guide to the development of a better understanding of the structure of nuclear and hadronic matter.

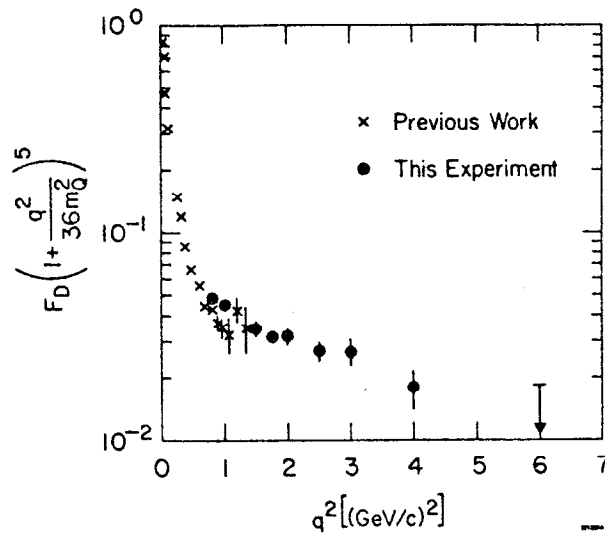


Fig. 11. Quark scaling prediction.

ACKNOWLEDGEMENTS

We extend our appreciation to Professor Wolfgang K. H. Panofsky for his interest and support of this investigation. We thank members of Group A and Dr. Robert Anderson for sharing with us their expertise, particularly with the spectrometers. We acknowledge the support of Dr. Charles Sinclair, Dr. David Sherden and the Spectrometer Facilities Group, and Professor Martin Perl for his support. Finally we should like to remember the late Professor Franz Bumiller for his assistance in providing the impetus in 1970 to initiate this investigation.

REFERENCES

1. R. Hofstadter and L. I. Schiff, eds., *Nucleon Structure: Proceedings Int. Conf. on Nucleon Structure, Stanford University, 1963* (Stanford University Press, 1964). The earliest work on eD elastic scattering was performed at Stanford in the range 0 to .14 GeV<sup>2</sup> by J. McIntyre and S. Dhar, *Phys. Rev.* 106, 1074 (1957).
2. W. Panofsky, in *Proc. Int. Conf. on Instrumentation for High Energy Physics (Dubna, 1970)*, Vol. 1, pp. 73-112; SLAC-PUB-798.
3. J. Elias, J. Friedman, G. Hartmann, H. Kendall, P. Kirk, M. Sogard, L. Van Speybroeck, and J. de Pagter, *Phys. Rev.* 177, 2075 (1969); refs. 1-9 therein are the earlier measurements of eD elastic scattering. See also S. Galster, H. Klein, J. Moritz, K. Schmidt, D. Wegener, and J. Bleckwenn, *Nucl. Phys.* B32, 221 (1971).
4. F. Gross, *Phys. Rev.* 142, 1025 (1966); 152, 1517E (1966); and M. Gourdin, *Nuovo Cimento* 28, 533 (1963).
5. The overlap integrals were kindly provided by Professor E. Lomon.
6. R. Reid, *Ann. Phys. (N. Y.)* 50, 411 (1968).
7. H. Arenhovel and H. Miller, *Z. Physik* 266, 13 (1974); V. Neudatchin, I. Obukhovskiy, V. Kukulin, and N. Golovanova, *Phys. Rev.* C11, 128 (1975); J. Vary, *Phys. Rev.* C7, 521 (1973).
8. M. Chemtob, E. Moniz, and M. Rho, *Phys. Rev.* C10, 344 (1974).
9. R. Adler and S. Drell, *Phys. Rev. Letters* 13, 349 (1964) and

- R. Adler, Phys. Rev. 141, 1499 (1966).
10. A. Jackson, A. Lande, and D. Riska, Phys. Letters 55B, 23 (1975).
  11. R. Blankenbecler and J. Gunion, Phys. Rev. D 4, 718 (1971).
  12. J. Gunion and L. Stodolsky, Phys. Rev. Letters 30, 345 (1973) and V. Franco, Phys. Rev. D 8, 826 (1973).
  13. S. Brodsky and G. Farrar, Phys. Rev. D 11, 1309 (1975).
  14. S. Brodsky, SLAC-PUB-1497, invited paper at Int. Conf. on Few Body Problems in Nuclear and Particle Physics, Quebec, 1974 (to be published).
  15. S. Stein, W. Atwood, E. Bloom, R. Cottrell, H. DeStaebler, C. Jordan, H. Piel, C. Prescott, R. Siemann, and R. Taylor, SLAC-PUB-1528, submitted to Phys. Rev.
  16. G. Miller, SLAC Report No. SLAC-129 (1971).
  17. W. Bartel, F. Büsler, W. Dix, R. Felst, D. Harms, H. Krehbiel, P. Kuhlmann, J. McElroy, J. Meyer, and G. Weber, Nucl. Phys. B58, 429 (1973).
  18. For original optics tests see Ref. 2; for refinement of 8 GeV coefficients see E. Riordan, Ph.D. dissertation, Appendix 1, MIT-LNS Report No. COO-3069-176.
  19. B. Gobbi, J. Rosen, H. Scott, S. Shapiro, L. Strawczynski, and C. Meltzer, Phys. Rev. Letters 33, 1450 (1974).
  20. R. Berard, F. Buskirk, E. Dally, J. Dyer, X. Maruyama, R. Topping, and T. Traverso, Phys. Letters 47B, 355 (1973).
  21.  $G_{EP}$  and  $G_{MP}$  are taken from F. Iachello, A. Jackson, and A. Lande, Phys. Letters 43B, 191 (1973),  $G_{EN}$  from S. Galster et al. in Ref. 3, and  $G_{MN}$  from Ref. 17 and K. Hanson, J. Dunning, M. Goitein, T. Kirk, L. Price, and R. Wilson, Phys. Rev. D 8, 753 (1973).
  22. F. Gross, Phys. Rev. D 10, 223 (1974), J. Hornstein and F. Gross, Phys. Letters 47B, 205 (1973), and F. Coester and A. Ostebee, Phys. Rev. C 11, 1836 (1975).
  23. D. Sivers, SLAC-PUB-1457. Submitted to Ann. Phys. (N.Y.).